Supplementary information

Figure S1 TLS derived non-intersecting screw axes are shown in a (**A**) side view and (**B**) bottom view for revTetR1 and (**D**) side view and (**E**) bottom view for the wild-type TetR-[Mg-TC]$^+$ complex (PDB ID: 1DU7). The length of each axis is proportional to the magnitude of libration along the axis. The origin is placed at the centre of reaction, which also corresponds to the centre of libration. (**C** and **F**) Fifty percent thermal ellipsoids. Direct viewing of the axes representing libration does not provide for an easy physical interpretation, in contrast the fifty percent thermal ellipsoid plot is indicative of the direction of motion.

TLS parameters provide an overall estimation of the degree of flexibility of individual domains in the context of the crystal. We are aware that such an analysis is biased by the number of crystal packing contacts in which the individual domains participate. Since all the structures we analyzed belong to different space groups, we counted the number of crystal contacts (atom separations between protein molecules smaller than 5.0 Å) that the DNA-binding domain (residues 6-46) participates in, in the different structures. The number of contacts for revTetR1-[Mg-ATC]$^+$, *tetO*-bound TetR, TetR-[Mg-TC]$^+$ and free TetR are 101, 142, 400 and 356, respectively. Therefore, the possibility exists that crystal packing influences the TLS parameters derived for the different structures. The figure was prepared with programs MOLSCRIPT (1) and RASTER3D (2).

1. Kraulis P (1991) MOLSCRIPT: a program to produce both detailed and schematic plots of protein structures. *Journal of Applied Crystallography* **24:** 946-950
2. Merritt EA, Bacon DJ (1997) Raster3D: Photorealistic molecular graphics. *Methods Enzymol.* **277:** 505–524

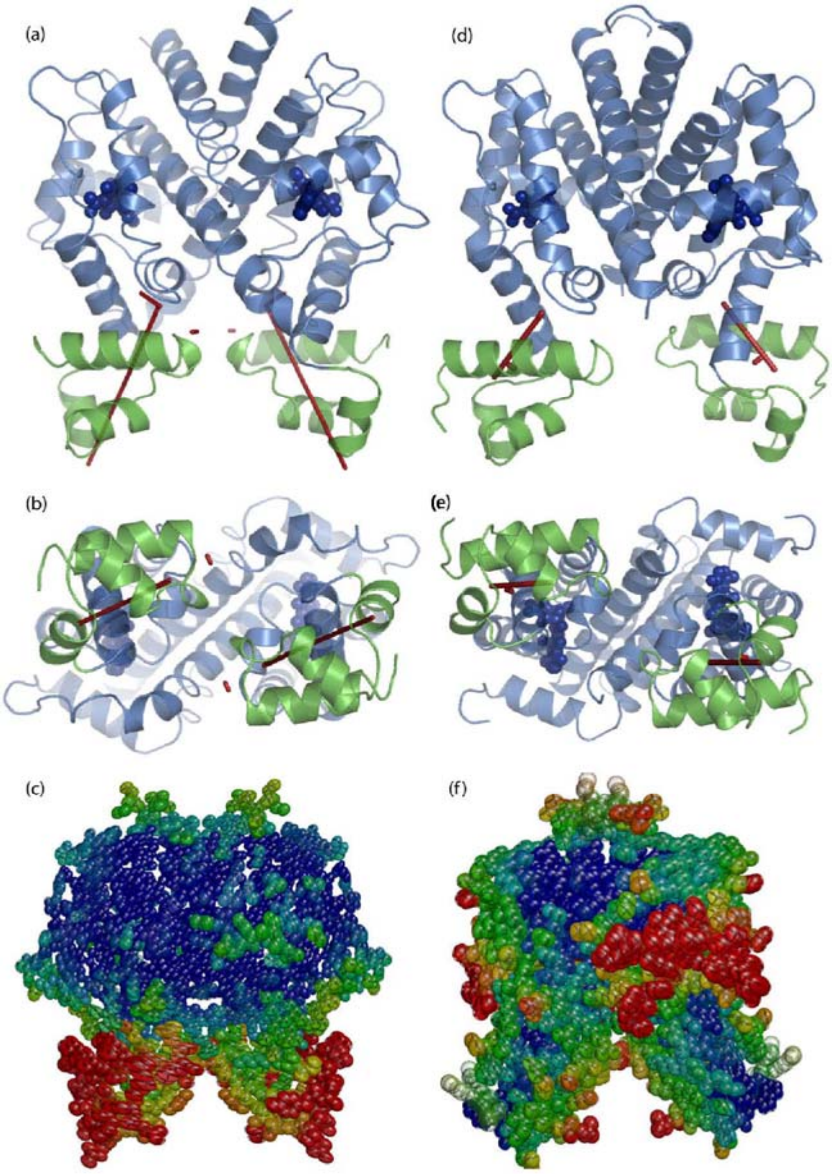

Supplementary Figure S1 (continued)

Table S1A Eigenvectors and Eigenvalues of the translation and libration tensors in ATC-bound revTetR1. The values are provided in the orthogonal coordinate system and using the centre of reaction as origin. This procedure minimizes T and makes S symmetric; domain definitions: D1: 6-45, D2: 46-91, D3: 92-161, D4: 162-205.

	T	**Direction cosines**	**Mean square t (Å^2)**	**L**	**Direction cosines**	**Mean-square l (°^{2})**
D1	1	0.896 0.122 -0.428	0.103	1	0.886 -0.463 0.034	1.058
	2	-0.065 0.987 0.146	0.184	2	0.415 0.758 -0.503	3.533
	3	0.440 -0.103 0.892	-0.061	3	0.207 0.459 0.864	25.227
D2	1	0.843 0.347 0.412	0.003	1	0.895 -0.256 0.364	0.954
	2	-0.032 0.796 -0.605	0.039	2	0.243 0.967 0.080	1.788
	3	-0.538 0.496 0.682	-0.006	3	-0.373 0.017 0.928	3.668
D3	1	0.708 -0.514 -0.484	0.006	1	0.812 -0.137 0.567	1.238
	2	0.352 0.851 -0.389	-0.016	2	0.437 0.787 -0.435	2.902
	3	0.612 0.105 0.784	0.023	3	-0.387 0.601 0.699	0.759
D4	1	0.862 -0.467 -0.196	-0.027	1	0.816 -0.485 0.315	0.562
	2	0.316 0.799 -0.512	0.010	2	0.568 0.772 -0.284	5.572
	3	0.396 0.380 0.836	0.005	3	-0.106 0.411 0.905	0.923

Table S1B Position of the non-intersecting screw axes and pitch of the screw motion about these axes in the revTetR1 structure using the centre of reaction as origin.

	S	Absolute position (x, y, z) (Å)	Pitch (Å)
D1	1	-29.702 -5.652 -3.891	-7.436
	2	-26.788 -0.644 -7.213	-5.516
	3	-26.825 -0.356 -7.367	1.084
D2	1	-27.437 -1.232 -24.223	4.749
	2	-31.336 3.603 -23.721	-3.719
	3	-24.786 2.810 -21.826	0.557
D3	1	-29.795 3.545 -25.164	2.321
	2	-30.595 2.222 -22.294	-0.553
	3	-36.842 -0.670 -23.913	-1.671
D4	1	-32.683 8.148 -16.781	4.474
	2	-34.283 -3.176 -28.226	0.547
	3	-39.945 -3.662 -27.163	-6.026

Table S1C Comparison between the mean square libration and pitch in the DNA-binding head of revTetR1, DNA-bound wild-type TetR (1QPI), Tc-bound wild-type TetR (1DU7) and Tc-free and DNA-free wild-type TetR (1A6I). The mean libration is equal to the trace divided by three.

	revTetR1	1QPI	1DU7	1A6I
Mean square displacement about axes of libration (°^{2})	1.058	7.647	0.937	0.289
	3.533	13.316	0.000	1.647
	25.227	1.182	11.530	9.514
Mean square libration (°^{2})	9.39	7.38	4.15	3.81
Pitch (Å)	-7.436	4.297	-7.824	-19.531
	-5.516	-1.962	0.000	-3.940
	1.084	-5.693	0.508	1.275